



Microbial Diversity and Sulfur Cycling in an Early Earth Analogue: From Ancient Novelty to Modern Commonality

C. Ryan Hahn,^a Ibrahim F. Farag,^{a*} Chelsea L. Murphy,^a  Mircea Podar,^{b,c} Mostafa S. Elshahed,^a  Noha H. Youssef^a

^aDepartment of Microbiology and Molecular Genetics, Oklahoma State University, Stillwater, Oklahoma, USA

^bDepartment of Microbiology, University of Tennessee Knoxville, Knoxville, Tennessee, USA

^cOak Ridge National Laboratory, Oak Ridge, Tennessee, USA

ABSTRACT Life emerged and diversified in the absence of molecular oxygen. The prevailing anoxia and unique sulfur chemistry in the Paleo-, Meso-, and Neoproterozoic and early Proterozoic eras may have supported microbial communities that differ from those currently thriving on the earth's surface. Zodletone spring in southwestern Oklahoma represents a unique habitat where spatial sampling could substitute for geological eras namely, from the anoxic, surficial light-exposed sediments simulating a preoxygenated earth to overlaid water column where air exposure simulates oxygen intrusion during the Neoproterozoic era. We document a remarkably diverse microbial community in the anoxic spring sediments, with 340/516 (65.89%) of genomes recovered in a metagenomic survey belonging to 200 bacterial and archaeal families that were either previously undescribed or that exhibit an extremely rare distribution on the current earth. Such diversity is underpinned by the widespread occurrence of sulfite, thiosulfate, tetrathionate, and sulfur reduction and the paucity of sulfate reduction machineries in these taxa. Hence, these processes greatly expand lineages mediating reductive sulfur-cycling processes in the tree of life. An analysis of the overlaying oxygenated water community demonstrated the development of a significantly less diverse community dominated by well-characterized lineages and a prevalence of oxidative sulfur-cycling processes. Such a transition from ancient novelty to modern commonality underscores the profound impact of the great oxygenation event on the earth's surficial anoxic community. It also suggests that novel and rare lineages encountered in current anaerobic habitats could represent taxa that once thrived in an anoxic earth but have failed to adapt to earth's progressive oxygenation.

IMPORTANCE Life on earth evolved in an anoxic setting; however, the identity and fate of microorganisms that thrived in a preoxygenated earth are poorly understood. In Zodletone spring, the prevailing geochemical conditions are remarkably similar to conditions prevailing in surficial earth prior to oxygen buildup in the atmosphere. We identify hundreds of previously unknown microbial lineages in the spring and demonstrate that these lineages possess the metabolic machinery to mediate a wide range of reductive sulfur processes, with the capacity to respire sulfite, thiosulfate, sulfur, and tetrathionate, rather than sulfate, which is a reflection of the differences in sulfur-cycling chemistry in ancient versus modern times. Collectively, such patterns strongly suggest that microbial diversity and sulfur-cycling processes in a preoxygenated earth were drastically different from the currently observed patterns and that the Great Oxygenation Event has precipitated the near extinction of a wide range of oxygen-sensitive lineages and significantly altered the microbial reductive sulfur-cycling community on earth.

KEYWORDS genome-resolved metagenomics, sulfur cycling, evolution, preoxygenated earth

Invited Editor Filipa L. Sousa, Univ. of Vienna

Editor Christa M. Schleper, University of Vienna

Copyright © 2022 Hahn et al. This is an open-access article distributed under the terms of the [Creative Commons Attribution 4.0 International license](https://creativecommons.org/licenses/by/4.0/).

Address correspondence to Noha H. Youssef, noha@okstate.edu.

*Present address: Ibrahim F. Farag, University of Delaware, Newark, Delaware, USA.

The authors declare no conflict of interest.

Received 7 January 2022

Accepted 14 February 2022

Published 8 March 2022

Sulfur is one of the most abundant elements on earth, exhibiting a wide range of oxidation states (-2 to $+6$). Microorganisms have evolved a plethora of genes and pathways for exploiting sulfur-redox reactions for energy generation. Reductive processes employ sulfur oxyanions or elemental sulfur as terminal electron acceptors in anaerobic respiratory schemes linked to heterotrophic or autotrophic growth. Oxidative processes, on the other hand, employ sulfides or elemental sulfur as electron donors, powering chemolithotrophic and photosynthetic growth.

Thermodynamic considerations limit reductive sulfur processes to habitats where oxygen is limited. This habitat restriction is reflected in the global distribution of microorganisms that reduce sulfate (SO_4^{2-}), sulfite (SO_3^{2-}), thiosulfate ($\text{S}_2\text{O}_3^{2-}$), tetrathionate ($\text{S}_4\text{O}_6^{2-}$), and elemental sulfur (S^0) (henceforth collectively referred to as SRM) in permanently and seasonally anoxic and hypoxic habitats in marine (1–3), freshwater (4), terrestrial (5), and subsurface (6) ecosystems. Sulfate is highly abundant on the current earth. Hence, sulfate reduction dominates reductive processes in the global sulfur cycle, although the reduction and disproportionation of the intermediate sulfur species, e.g., sulfur (7, 8), sulfite (8), thiosulfate, and tetrathionate (9, 10), could be significant in localized settings.

The history of earth's sulfur cycle is a prime example of a geological-biological feedback loop, where the evolution of biological processes is driven by, and dramatically impacts, the earth's biogeochemistry. The earth's surface was completely anoxic during the first two billion years of its history, and the availability and speciation of various sulfur species differed greatly from their current values. Sulfate levels were significantly lower than to current values in oceanic water (28 mM), with estimates of $<200 \mu\text{M}$ to 1 mM from the Archean up to the Paleoproterozoic (2.3 gigayears ago [Gya]) eras (11–14). On the other hand, intermediate sulfur species appear to have played an important role in shaping the ancient sulfur cycle (15). Modeling suggests that mM levels of SO_3^{2-} were attained in the Archean anoxic shallow surficial aquifers as a result of the dissolution of the volcanic SO_2 prevailing in aquatic habitats (12). Isotopic studies have demonstrated the importance of elemental sulfur, sulfite, and thiosulfate reduction in the Archean era (15, 16).

The evolution of life (3.8 to 4.0 Gya) in the early Archean era and the subsequent evolution of major bacterial and archaeal clades in the late Archean and early Proterozoic eras (17) occurred within this background of anoxia and characteristic sulfur chemistry. As such, it has been speculated that organisms using intermediate forms of sulfur were likely more common than sulfate-reducing organisms (15). However, while isotopic fractionation, modeling, and microscopic studies could provide clues on prevailing sulfur speciation patterns and prevalent biological processes, the identity of microorganisms mediating such processes is unknown. This knowledge gap is due mostly to constraints on the preservation of nucleic acids and other biological macromolecules, with the oldest successful DNA-sequenced sample being only 1.2 million years old (18).

Investigation of the microbial community in modern ecosystems with conditions resembling those prevailing in the ancient earth could provide important clues to the nature and identity of microorganisms that thrived under conditions prevailing prior to earth's oxygenation. In Zodletone spring, a surficial anoxic spring in southwestern Oklahoma, anoxic, surficial, light-exposed conditions are maintained in the sediments by the constant emergence of sulfide-saturated water at the spring source from anoxic underground water formations in the Anadarko Basin, along with gaseous hydrocarbons, which occur in seeps in the general vicinity. These surficial anoxic conditions also support a sulfur chemistry characterized by high levels of sulfide, sulfite, sulfur (soluble polysulfide), thiosulfate, and a low level of sulfate, as reported previously (19–21). Microbial diversity using 16S rRNA amplicon surveys have reported a higher level of phylogenetic diversity in the anoxic spring sediments and the affiliation of a fraction of the spring community with previously recognized sulfur-metabolizing lineages, as well as the high proportion of phylogenetically novel taxa in the spring anoxic sediments (20, 22, 23). As such, the prevailing conditions at the spring source are reminiscent of

ancient metabolic capacities prevailing on the earth's surface in the late Archean/early Proterozoic eras as noted previously (19).

Furthermore, the sediments at the source of the spring are overlaid by an air-exposed water column, and prior microsensor measurements and detailed geochemical analysis (19, 21) demonstrated that oxygen intrusion leads to a vertical oxygen gradient (from oxic in the top 1 μm , to hypoxic in the middle, to anoxic in deeper layers overlaying the sediments) (see Fig. S1 in the supplemental material). As such, contrasting communities between the anoxic sediments and the oxygen-exposed water column could provide a glimpse into how oxygen evolution has altered such communities. Here, we combined metagenomic, metatranscriptomic, and amplicon-based approaches to fully characterize the microbial community in Zodletone spring. Our results provide a glimpse of the community mediating the ancient sulfur cycle, significantly expand the overall microbial diversity by the description of a wide range of novel lineages, and greatly increase the number of lineages documented to mediate reductive sulfur processes in the microbial tree of life.

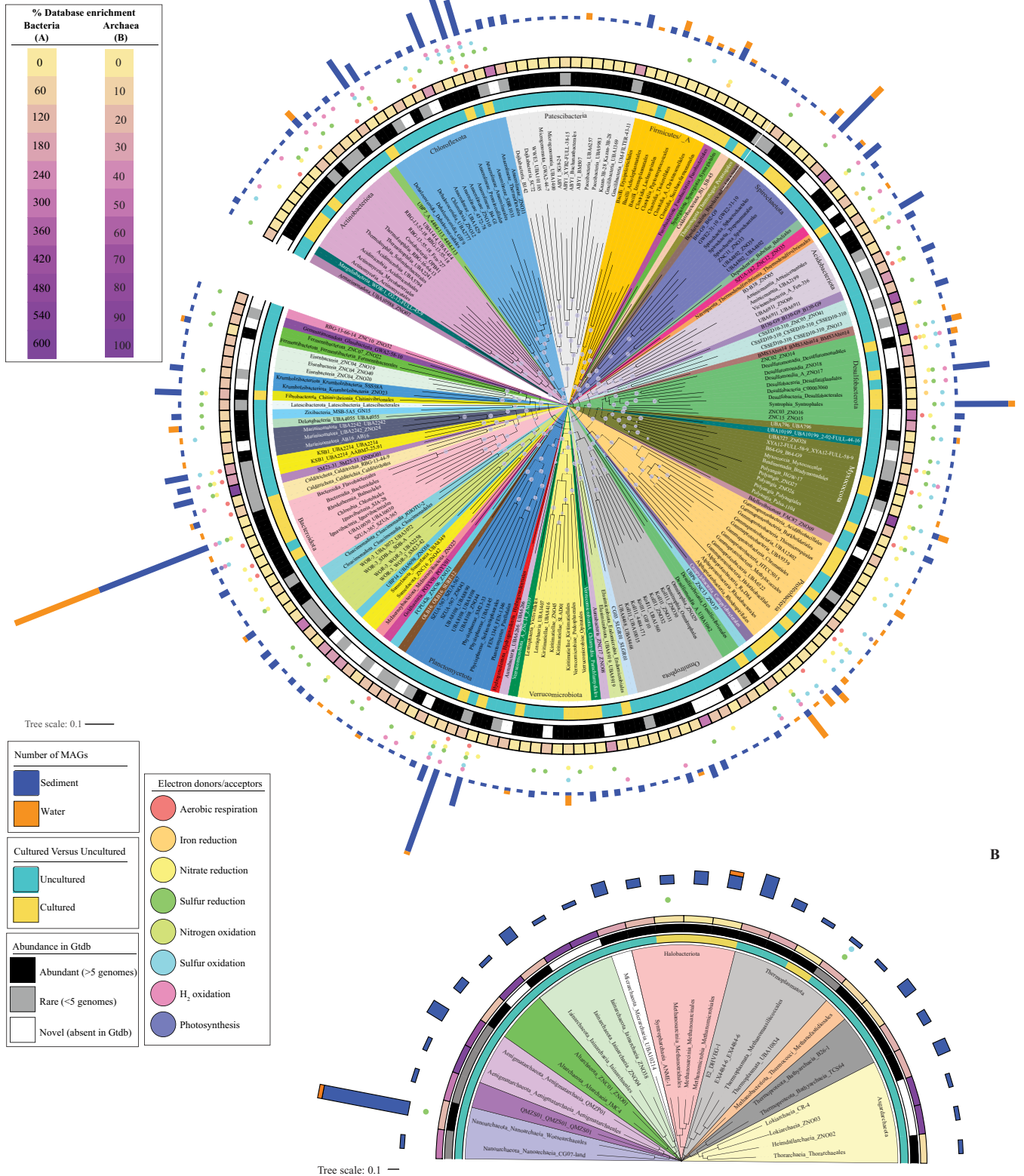
RESULTS

Novel phylogenetic diversity in Zodletone sediments. Metagenomic sequencing of the spring sediments yielded 281 Gbp, of which 79.54% assembled into 12-Gbp contigs, with 6.8-Gbp contigs longer than 1 Kbp. A total of 1,848 genomes were binned, but only 683 passed quality-control criteria, and 516 remained after dereplication (see Table S1 in the supplemental material). These metagenome-assembled genomes (MAGs) represented 64 phyla or candidate phyla (53 bacterial and 11 archaeal), 127 classes, 198 orders, and 300 families (Fig. 1A and B). A diversity assessment utilizing small subunit ribosomal protein S3 from assembled contigs ($n = 2,079$), as well as a complementary 16S rRNA Illumina sequencing effort ($n = 309,074$ amplicons), identified a higher number of taxa (82 phyla and 1,679 species in the ribosomal protein S3 data set, and 69 phyla and 1,050 species in 16S rRNA data set) (see Fig. S2 in the supplemental material). Nevertheless, the overall community composition profiles generated from all three approaches were broadly similar (Fig. S2), suggesting that the MAG list largely reflects the sediment microbial community.

An assessment of the novelty and degree of uniqueness of sediment MAGs identified a remarkably high number of previously undescribed lineages (1 phylum, 14 classes, 43 orders, and 97 families) as well as lineages exhibiting rare global distribution (LRD) pattern (11 phyla, 24 classes, 45 orders, and 113 families) in the spring (Fig. 1 to 3). We define LRD lineages as those represented by 5 genomes or less in the Genome Taxonomy Database release 95 (GTDB r95). At the family level, 132 (25.58%) and 208 (40.03%) genomes clustered into 97 novel and 113 LRD families, respectively, bringing the proportion of genomes belonging to novel or LRD families in Zodletone sediments to 65.89%. The high level of novelty in the sediment MAGs is reflected in an average relative evolutionary divergence (RED) value of 0.76, which is a value that is slightly lower than the median RED value for the designation of a novel family (0.77) (24).

The *Chloroflexota* ($n = 69$), *Planctomycetota* ($n = 47$), *Bacteroidota* ($n = 43$), *Desulfobacterota* ($n = 43$), *Spirochaetota* ($n = 28$ genomes), *Patescibacteria* ($n = 20$ genomes), and the archaeal phylum *Nanoarchaeota* ($n = 21$) were the most abundant phyla in Zodletone spring sediments, albeit representing only 52.52% of the total number of recovered genomes (see Text S1 in the supplemental material; Fig. 1 and 3; see Fig. S3 in the supplemental material). An extreme paucity of genomes belonging to the *Proteobacteria* (6 genomes) and *Firmicutes* (12 genomes), which are widely distributed and abundant taxa in current biomes (25), and the absence of oxygen-generating *Cyanobacteria* (0 genomes) were observed (Fig. 1, Fig. S3). Therefore, in addition to expanding the number of novel lineages (classes, orders, and families) and greatly enriching available genomes in rare, poorly represented taxa, our results highlight the uniqueness and distinction of the microbial community thriving in Zodletone spring sediments, compared with those of present earth environments studied so far.

A



B

FIG 1 Phylogenomics of the 516 bacterial (A) and 114 archaeal (B) genomes analyzed in this study. The maximum likelihood trees were constructed in FastTree (86) based on the concatenated alignments of 120 (bacterial), and 122 (archaeal) housekeeping genes obtained from GTDB-TK (85). The branches represent order-level taxonomy and are color coded by phylum. For phyla with 4 orders or less, branches are labeled as Phylum_Class_Order. For phyla with more than 4 orders, the phylum is shown at the base of the colored wedge and the branches are labeled as Class_Order. Lineages starting with ZN depict novel lineages (ZNC, novel class; ZNO, novel order). Bootstrap support values are shown as bubbles for nodes with >70% support. Tracks around (Continued on next page)

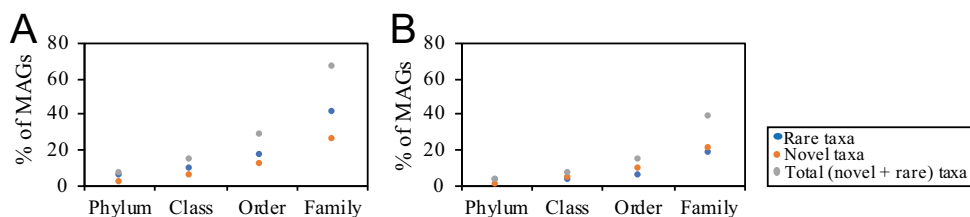


FIG 2 Novelty, rarity, and phylum-level makeup in Zodletone sediment and water communities. Genomes belonging to novel (orange), and LRD (blue) lineages are shown as a percentage of total binned genomes in the sediment (A) and the water (B) communities. The sum of novel and LRD genome percentages is shown in gray.

Oxygen intrusion reduces the proportion of novel and rare lineages in Zodletone spring.

Metagenomic sequencing of the oxygen-exposed overlying water column community yielded 323 Gbp, of which 80.07% assembled into 3.6-Gbp contigs, with 3.1-Gbp contigs of >1 Kbp. A total of 883 genomes were binned, with only 114 remaining after dereplication. Of these genomes, 62 belonged to families shared with the sediment community, while 52 were water specific. Genomes recovered from the water column belonged to a significantly lower number of phyla ($n = 27$), classes ($n = 37$), orders ($n = 52$), and families ($n = 79$) than those from the euxinic sediments (Table S1). The community exhibited a much lower level of novelty and rarity at the phylum, class, order, and family levels than those of the sediment community (Fig. 2). Water-specific genomes ($n = 52$) belonged mostly to well-characterized microbial lineages, e.g., families *Rhodobacteraceae* and *Rhodospirillaceae* in *Alphaproteobacteria*; families *Thiomicrospiraceae*, *Halothiobacillaceae*, *Acidithiobacillaceae*, *Burkholderiaceae*, *Chromatiaceae*, and *Methylothermaceae* in *Gammaproteobacteria*; families *Sulfurimonadaceae* and *Sulfurovaceae* in phylum *Campylobacterota*; and well described families in the phyla *Bacteroidota* and *Desulfobacterota* (Text S1; Fig. 1; Table S1). Collectively, this information demonstrates a pattern where the intrusion of oxygen is negatively correlated with the presence of previously undescribed and LRD lineages, which are prevalent in the sediment.

Reductive sulfur processes dominate Zodletone spring sediment communities.

A total of 149 genomes (28.9% of all genomes), belonging to 32 phyla, 51 classes, 69 orders, and 97 families were involved in at least 1 reductive sulfur processes (Fig. 4; see Fig. S4 and Table S2 in the supplemental material). By comparison, only 21 sediment genomes (4.06% of all genomes) encoded at least 1 sulfur oxidation pathway (Fig. 4, Fig. S4; Table S2). The reductive sulfur community in the spring exhibited two unique traits as follows: first, a majority of genomes encoding such capacities belonged to novel (47 genomes) or LRD (66 genomes) lineages (Fig. 4, Fig. S4), and second, sulfite, polysulfide, thiosulfate, and tetrathionate reduction capacities appear to be more prevalent than sulfate-reduction capacities in the sediment genomes.

Sulfate reduction capacity was encoded in only 18 sediment genomes (Fig. 4, Fig. S4) but exhibited a unique community composition, when compared with well-studied marine and terrestrial habitats (1, 2, 4, 26). Sulfate reduction capacities were observed in mostly previously undescribed or LRD lineages within the *Zixibacteria*, *Acidobacteriota* (members of family UBA6911, equivalent to *Acidobacteria* group 18), *Myxococcota*, *Bacteroidota*, *Planctomycetota*, and candidate phylum OLB16 (1 genome),

FIG 1 Legend (Continued)

the tree represent (from innermost to outermost) the following: cultured status at the order level (cultured versus uncultured), abundance in GTDB based on the number of available genomes (abundant with more than 5 genomes, rare with 5 genomes or less, and novel with no genomes in GTDB), percentage database enrichment (calculated as number of genomes belonging to a certain order binned in the current study as a percentage of the number of genomes belonging to the same order in GTDB), energy conservation capabilities depicted by colored circles (salmon, aerobic respiration; orange, Fe^{3+} respiration; yellow, nitrate/nitrite reduction; dark green, reductive sulfur processes; lime green, nitrogen oxidation; cyan, oxidative sulfur processes; pink, respiratory hydrogen oxidation; and purple, photosynthesis), and the number of MAGs belonging to each order binned from the sediment (blue bars) and the water (orange bars). For orders with 20 or more genomes, the family-level delineation is shown in Fig. 3. These orders are *Anaerolineales* (Fig. 3A), *Bacteroidales* (Fig. 3B), *Sedimentisphaerales* (Fig. 3C), *Spirochaetales* (Fig. 3D), *Syntrophales* (Fig. 3E), and *Woeseearchaeales* (Fig. 3F).

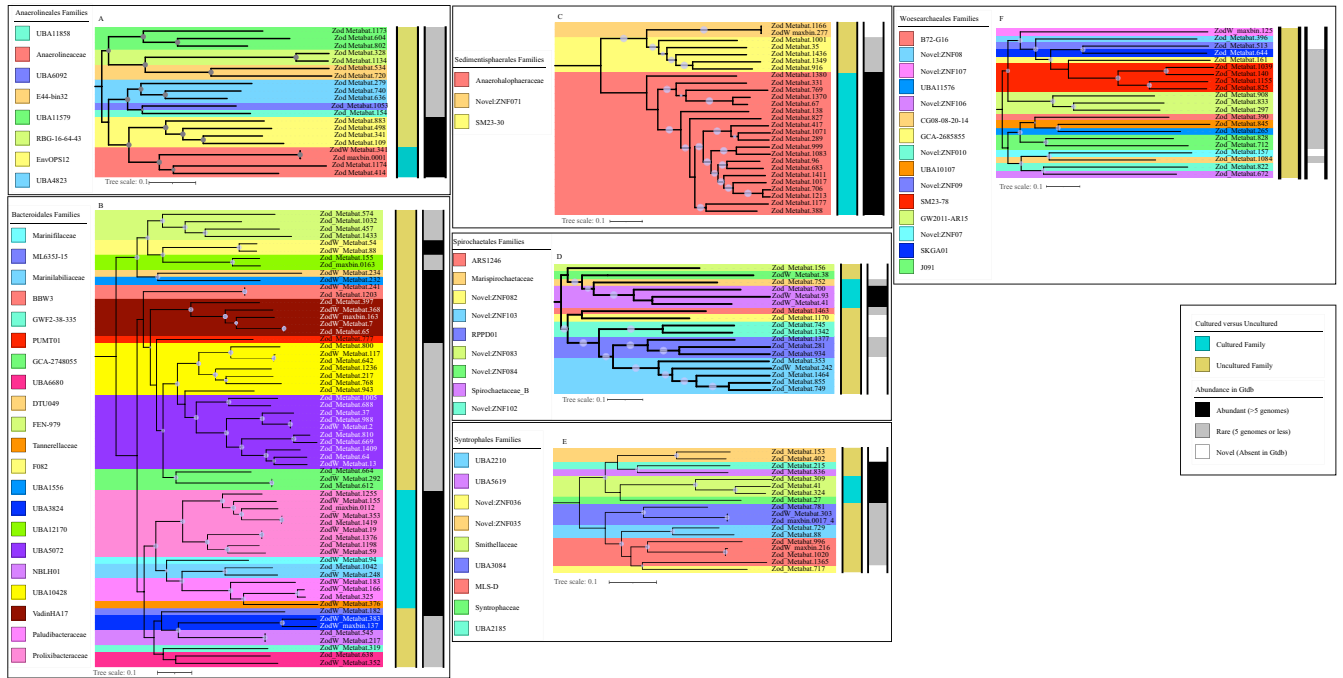


FIG 3 Family-level delineation for orders with 20 or more genomes. The maximum likelihood trees were constructed in FastTree (86) based on the concatenated alignments of 120 and 122 single-copy genes obtained from GTDB-TK (85). Bootstrap support values are shown as bubbles for nodes with >70% support. Families are color coded. To the right of the trees, tracks are shown for cultured status at the family level (cultured versus uncultured) and abundance in GTDB based on the number of available genomes (abundant with more than 5 genomes, rare with 5 genomes or less, and novel with no genomes in GTDB).

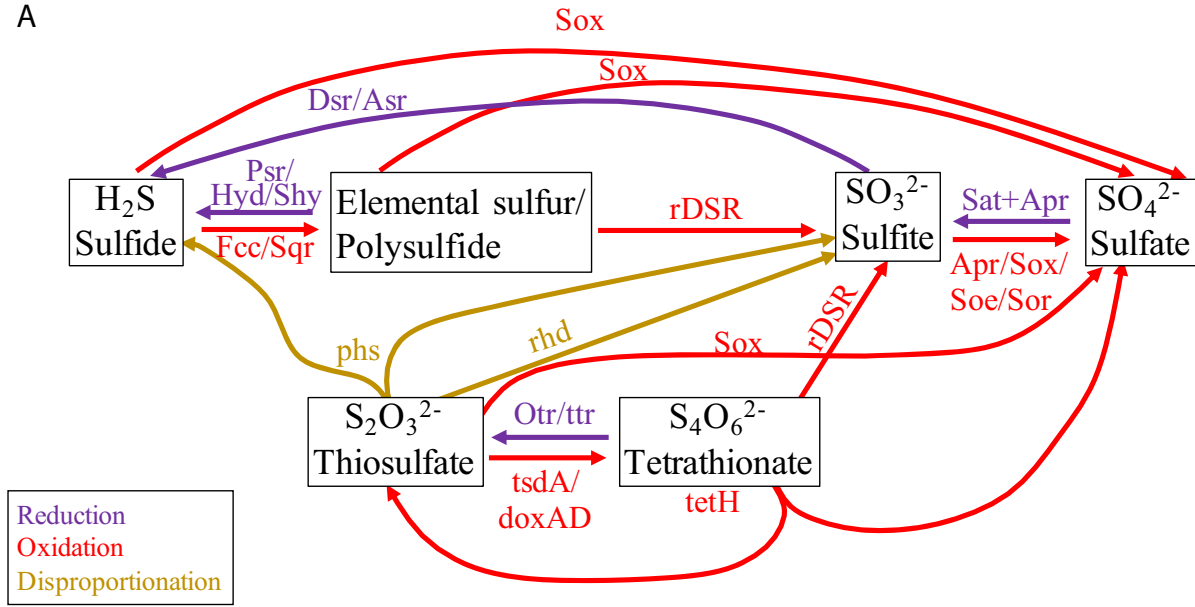
as well as rare and novel lineages within *Desulfobacterota* (Fig. 4, Fig. S4; see Fig. S5a in the supplemental material; Table S2).

Sulfite (but not sulfate) reduction via the DsrAB+DsrC+DsrKMJOP system was identified in only 8 genomes belonging to 7 families within the phyla *Planctomycetes*, *Chloroflexota*, *Spirochaetota*, and *Desulfobacterota* (Fig. 4, Fig. S4 and S5b; see Fig. S6a in the supplemental material; Table S2). On the other hand, the sulfite reduction capacity within Zodletone spring sediment solely via the Asr/Hdr system was rampant, being encountered in 104 genomes belonging to 28 phyla, 43 (8 novel and 9 LRD) classes, 56 (18 novel and 12 LRD) orders, and 72 (31 novel and 25 LRD) families (Fig. 4, Fig. S4 and S6b; Table S2), with a gene organization of the *asr* locus adjacent to the *hdr* locus in the majority of genomes (Fig. S6b). *Asr*-encoding genomes in the sediment included members of previously undescribed and LRD lineages within the *Chloroflexota*, *Desulfobacterota*, *Planctomycetota*, and *Bacteroidota*. The capacity was also rampant in the yet-uncultured bacterial phyla, of which many have a fairly limited global distribution (e.g., the candidate phyla CSSED10-310, FCPU426, RBG-13-66-14, SM23-31, SZUA-182, UBP14, *Aureabacteria*, *Sumerlaeota*, and *Krumholzibacteriota*). Zodletone dissimilatory sulfite reductase (Fig. S6a) and the anaerobic sulfite reductase (Fig. S6b) sequences clustered with reference sequences from the same phylum, generally showing no evidence of LGT.

Sulfur (polysulfide) reduction capacities were observed in 20 Zodletone sediment genomes that encoded *psrABC* genes (Fig. 4, Fig. S4, S5c, and S6c; Table S2). In addition, representatives of the cytoplasmic sulfurhydrogenase I (HydABCD system) and/or II (ShyABCD system) were identified in 119 Zodletone sediment genomes (Fig. 4). However, the direct involvement of these enzymes in an ETS-associated respiration is not yet clear (Text S1).

Sediment genomes also encoded thiosulfate disproportionation and reduction capacities. The quinone-dependent membrane-bound molybdopterin-containing thio-sulfate reductase PhsABC was encoded in 11 genomes belonging to 6 phyla (Table S2;

A



B

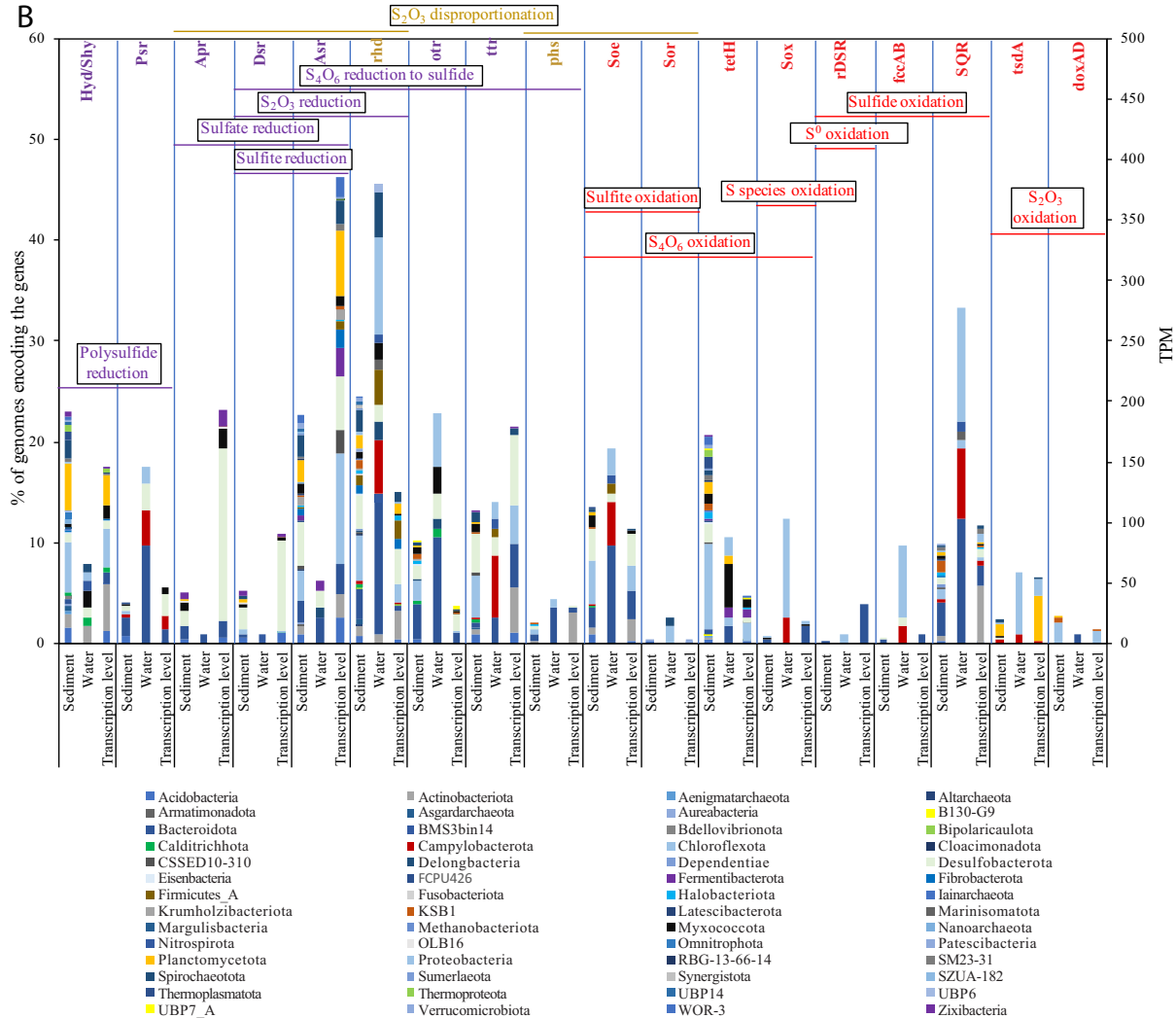


FIG 4 Sulfur cycle in Zodlstone spring. (A) Diagram of sulfur transformations predicted to take place in the spring. Different sulfur species are shown in black boxes. Reduction reactions are depicted by purple arrows, oxidation reactions are depicted by red arrows, while (Continued on next page)

Fig. S6d). Within these genomes, only two (a *Chloroflexota* family UBA6092 genome and a *Desulfatiglandales* family HGW15 genome) also encoded a dissimilatory sulfite reductase (the Asr system) akin to the *Gammaproteobacteria* thiosulfate-disproportionating pure culture members (27), where the final products of thiosulfate disproportionation are expected to be only hydrogen sulfide (Fig. 4, Fig. S4 and S5d; Table S2). On the other hand, 5 of the 11 phsABC-encoding Zodletone genomes also encoded the sulfite dehydrogenase SoeABC system, akin to *Desulfobacterota* and *Firmicutes* pure culture members, where the final products of thiosulfate disproportionation are expected to be both hydrogen sulfide and sulfate (28, 29) (Fig. 4, Fig. S4 and S5d; Table S2).

In addition to the phsABC system, 14 Zodletone genomes belonging to 6 phyla encoded a rhodanase-like enzyme (EC 2.8.1.1 or EC 2.8.1.3) for thiosulfate disproportionation, as well as enzymes for both sulfite oxidation (by means of reversal of sulfate reduction via Sat+AprAB or the sulfite dehydrogenase SoeABC), and sulfite reduction (via the dissimilatory sulfite reductases Dsr or Asr), where the final products of thiosulfate disproportionation are expected to be both hydrogen sulfide and sulfate (30–34) (Fig. 4, Fig. S4 and S5d; Table S2).

Tetrathionate reduction capacities were identified in 105 sediment genomes. Seventy-three Zodletone sediment genomes from 14 phyla encoded the octaheme tetrathionate reductase (OTR) enzyme (Table S2; Fig. 4, Fig. S4 and S6e). In addition to Otr, 68 Zodletone genomes from 14 phyla encoded the Ttr enzyme system (Table S2; Fig. 4, Fig. S4 and S5e). As shown previously in *Salmonella enterica* serovar Typhimurium (27), in the presence of means for thiosulfate disproportionation/reduction and sulfite reduction, the thiosulfate produced as a result of tetrathionate reduction could be further reduced to sulfide. Out of the 105 sediment genomes encoding the Otr, and/or Ttr enzymes, only 12 genomes also encoded thiosulfate and sulfite reduction enzymes.

Within lineages mediating reductive sulfur processes in Zodletone sediments ($n = 98$), a wide range of substrates supporting sulfidogenesis were identified (Table S3; Fig. S4). They included hexoses (26% to 87% of sulfidogenic lineages); pentoses (30% to 41% of sulfidogenic lineages); amino acids and peptides (39% of lineages); short-chain fatty acids, e.g., lactate, propionate, butyrate, and acetate (22% to 73% of lineages); long-chain fatty acids (29% of lineages); aromatic hydrocarbons (3% of lineages); and short-chain alkanes (6% of lineages). Autotrophic capacities with hydrogen as the electron donor were identified in 28% of sulfidogenic lineages.

Transcriptomic analysis. Transcriptomic expression of genes involved in S species reduction/disproportionation was analyzed in the spring sediments (Fig. 4). All S species reduction/disproportionation genes discussed above were identified and mapped to 51 distinct phyla. Total transcription levels of the Asr system were 4 times higher than those of the Dsr system, which is consistent with the higher number of Zodletone sediment genomes encoding the Asr system than that of the Dsr system. Asr system genes were mapped to 11 phyla; while DSR genes mapped to 4 phyla (Fig. 4). Sulfate reduction genes (Sat, AprAB, and QmoABC) were also transcribed with major contributions from 4 phyla. Transcription of the thiosulfate disproportionating rhodanese-like (EC 2.8.1.1 or EC 2.8.1.3), thiosulfate reductase *phsABC*, tetrathionate reduction genes *ttrABC*, octaheme tetrathionate reductase *otr*, *psrABC* for polysulfide reduction, and cytoplasmic sulfurhydrogenases I and II (*hyd/shy* systems) were also identified (Fig. 4; Text S1, for detailed contributions of taxa).

Oxidative sulfur processes dominate the Zodletone water community. Reductive sulfur processes were extremely sparse in the water community (Fig. 4, Fig. S4; Table S2; Text S1). In contrast, oxidative sulfur processes dominated the water commu-

FIG 4 Legend (Continued)

disproportionation reactions are depicted by golden-brown arrows. The gene names are shown on the arrows. (B) Phylum-level distribution of the S cycling genes shown at the top of the figure in sediment and water genomes, as well as the transcriptomic data set. Processes involving more than one gene are highlighted by horizontal bars and are color coded by reduction (purple), oxidation (red), or disproportionation (golden brown), with the name of the process shown on top of the horizontal bar. RNA-seq reads were pseudoaligned to the S cycling genes predicted in Zodletone genomes to detect exact matches using Kallisto (95). The transcripts per million are shown on the secondary y axis for the gene/group of genes depicted at the top of the figure.

nity, with pathways encoding sulfide, sulfur, thiosulfate, tetrathionate, and/or sulfite oxidation to sulfate present in 59/114 (51.8%) of water genomes, belonging to 13 phyla, 16 classes, 25 orders, and 43 families, respectively. The oxidative sulfur community in the water belonged to mostly well-characterized lineages (Table S2; Fig. 4, Fig. S4), with only 8 and 10 genomes involved in oxidative sulfur processes belonging to previously undescribed and LDR families, respectively. A complete SOX system, putatively mediating oxidation of a wide range of reduced sulfur-species to sulfate, was encoded in genomes belonging to well-characterized families within *Proteobacteria* (11 genomes in *Acidithiobacillaceae*, *Burkholderiaceae*, *Halothiobacillaceae*, *Rhodobacteraceae*, and *Thiomicrospiraceae*) and *Campylobacterota* (3 genomes in the family *Sulfurimonadaceae*) (Table S2; Fig. 4, Fig. S4). The capacity for sulfide oxidation to sulfur (sulfide dehydrogenase and/or the sulfide:quinone oxidoreductase Sqr) was encoded in 39 water genomes (Text S1; Table S2; Fig. 4, Fig. S4). Only 2 of the above 39 genomes (a *Proteobacteria* genome and a *Nitrospirota* genome) encoded the capacity to further oxidize the sulfur/polysulfide to sulfite via the reversal of the Dsr system. The capacity for sulfite oxidation to sulfate via the reversal of AprAB+QmoABC system, the sulfite dehydrogenase (quinone) SoeABC, or the sulfite dehydrogenase (cytochrome) SorAB system was encoded in 1, 22, and 3 genomes, respectively (Text S1; Table S2; Fig. 4, Fig. S4). Finally, for thiosulfate oxidation, eight water genomes (*Proteobacteria* and *Flavobacteriaceae*) encoded thiosulfate to tetrathionate oxidation capacities via either the thiosulfate dehydrogenase *tsdA* (EC 1.8.2.2) or *doxAD* (EC 1.8.5.2). Two of these 8 genomes also encoded tetrathionate hydrolase (*tetH*) (35) that is known to cleave tetrathionate to thiosulfate, sulfur, and sulfate (Text S1; Table S2; Fig. 4, Fig. S4). Simultaneous identification of the SOX system and both forms of sulfide dehydrogenase (*fccAB* and Sqr) imply that these two genomes encode the capacity for complete thiosulfate oxidation to sulfate.

DISCUSSION

The microbial community in Zodletone spring sediments exhibited a high level of phylogenetic diversity, novelty, and rarity (Fig. 1 to 3, Fig. S3). Conversely, representatives of lineages that predominate in most present earth environments, e.g., *Proteobacteria*, *Firmicutes*, and *Cyanobacteria*, were absent or extremely sparse within the sediments. The community in the spring sediments was also characterized by a high proportion of SRM and the prevalence of lineages mediating the reduction of sulfur cycle intermediates (sulfite, thiosulfate, tetrathionate, and elemental sulfur) over sulfate reducers. Many of the organisms mediating reductive sulfur-cycling processes belonged to novel and LRD lineages (Fig. S4), hence expanding the range of SRM within the tree of life (Fig. S5).

What drives the assembly, propagation, and maintenance of such a diverse, novel, and distinct community in the spring sediments? The high level of diversity, novelty, and rarity within Zodletone spring sediment SRM community could be attributed to two main factors. First, a wide range of sulfur cycle intermediates are available in concentrations much higher than sulfate, in contrast to sulfate predominance in current ecosystems (2). Such a pattern selects for a more diverse community of SRM in the spring than that of predominantly sulfate-driven marine and freshwater ecosystems (Fig. S4). Second, additional factors usually constraining SRM growth in several habitats, such as diel or seasonal intrusion of oxygen, Fe and NO₃ (1, 36–38), recalcitrance of available substrates (6, 39, 40), temperature (41, 42), pH (26, 43, 44), salinity (45), and pressure extremes (39, 46), or combinations thereof, are absent in the spring. Therefore, while the reductive global sulfur cycle appears to be dominated by a few sulfate-reducing lineages within *Desulfobacterota*, and to a lesser extent *Firmicutes*, as well as *Thermodesulfobacteria* and *Archaeoglobus* in high-temperature habitats, the SRM community in Zodletone is extremely diverse, encompassing a wide range of previously undescribed and LRD lineages (Fig. 4, Fig. S4, S5, and S6).

Sulfate-reducing organisms are the most prevalent component of the reductive sulfur cycle in most marine and aquatic ecosystems. Aspects of the ecology (2),

physiology (47), and biochemistry (48–50) of dissimilatory sulfate reduction have been investigated extensively (51). While not the most prevalent process, the sulfate-reducing community in Zodletone spring sediment exhibited a unique composition, with members of *Zixibacteria*, *Acidobacteriota*, *Myxococcota*, *Bacteroidota*, *Planctomycetota*, and candidate phylum OLB16 constituting the major players, as well as rare and novel lineages within *Desulfobacterota* (*Desulfatiglandales* and order C00003060), with scarce representation of canonical *Desulfobacterota* sulfate reducers (1 genome). While the identification of the dissimilatory sulfate-reducing machinery in some of these lineages (e.g., *Zixibacteria*, *Acidobacteriota*, and *Planctomycetota*) has been shown before (52–54), these members rarely appear to be the dominant players in a single ecosystem.

Compared with sulfate reduction, the ecology and diversity of microbial dissimilatory sulfite reduction has not been studied extensively. The biochemistry of the process has been examined in sulfate reducers, when grown on sulfite (51), as well as in a few other dedicated sulfite reducers, such as members of *Desulfitobacterium* (55), *Salmonella* (56), *Shewanella* (57), and *Wolinella* (58). A recent study suggested the importance and the ancient nature of sulfite reduction in an extreme thermophilic environment in a limited diversity biofilm (59). We document a plethora of microorganisms within the phyla *Planctomycetes*, *Chloroflexota*, *Spirochaetota*, and *Desulfobacterota* encoding the dissimilatory sulfite reductase DSR, as well as 72 additional families (31 novel and 25 LRD) encoding the anaerobic sulfite reductase. These organisms expand the known sulfite reduction capacity within the domain *Bacteria* (Fig. S5). Furthermore, the novelty or rarity of some of these families is a reflection of the dearth of current habitats that could support this mode of metabolism, once predominant on ancient earth.

The bulk of knowledge on thiosulfate reduction and or disproportionation comes from studies in pure cultures, e.g., members of *Desulfobulbaceae* (e.g., *Desulfocapsa*) (28, 60) and the genera *Desulfovibrio* and *Desulfomonile* (61–63) within *Desulfobacterota*, the gammaproteobacterium *Pantoea agglomerans* (64), and members of *Thermodesulfobacteria* (65) and *Firmicutes* (29). Radioisotope tracing of different sulfur atoms showed a significant contribution of thiosulfate disproportionation to the sulfur cycle in marine (66), as well as freshwater, sediments (67). However, the lack of a marker gene for the process hinders ecological culture-independent studies. Similar to sulfite, the high levels and constant generation of thiosulfate in Zodletone sediments sustain a highly diverse thiosulfate-reducing (thiosulfate reductase plus a sulfite reduction complex) or thiosulfate-disproportionating (thiosulfate reductase plus both sulfite reduction and sulfite oxidation systems) community with major contributions from novel or rare families in *Acidobacteriota*, *Chloroflexota*, *Desulfobacterota*, KSB1, *Myxococcota*, and *Spirochaetota*. Finally, the extremely high levels of zero valent sulfur, available as soluble polysulfide, result in enriching the community with a plethora of polysulfide-reducing organisms.

As described above, this study infers that the microbial communities thriving under ancient conditions of anoxia and a high proportion of sulfur cycle intermediates were extremely diverse. In comparison, communities in the oxygen-exposed water column were markedly less diverse. What drives this drastic shift in diversity and community structure? We argue that oxygen introduction into the system is responsible for such a shift, as evident by the shift to oxidative sulfur processes in the water samples. The prevailing conditions in the water column are hence more akin to microbial communities that would thrive in sulfur-rich yet air-exposed habitat on the current earth.

The comparison presented here between both communities could demonstrate putatively how ancient metabolic pathways and lineages mediating them have been curtailed due to oxygen evolution and predominance in the current surficial earth. The evolution of oxygenic photosynthesis has led to the steady and inexorable accumulation of O₂ in Earth's atmosphere (the great oxidation event [GOE]), with the rise of atmospheric O₂ to 1% to 5% of current levels between 2.4 and 2.1 billion years (Gyr) ago, and its accumulation to values comparable to modern values 500 to 600 million years ago (Mya) (68). Due to the expected sensitivity and lack of adaptive mechanisms to cope with atmospheric oxygen in multiple strict anaerobes, as well as the chemical

instability of multiple *S* species in an oxygenated atmosphere, the GOE exerted a profound negative impact on anaerobic surficial life forms (the oxygen catastrophe) leading to the first and arguably most profound extinction event in earth's history (68). In addition to suppressing anaerobiosis in atmospherically exposed habitats, the GOE also led to a significant change in the *S* cycle, from one based on atmospheric inputs to one dependent on oxidative weathering leading to the release of a huge amount of sulfate derived from the oxidation of pyrite and the dissolution of sulfate minerals (69), hitherto a minor by-product of Archean abiotic and biotic reactions (15, 70). Therefore, it appears that the loss of niches associated with geological transformations could be one of the possible explanations for high extinction rates for microorganisms on earth, as well as the constant identification of rare, novel taxa within anaerobic settings. It is notable that phylogenetically novel branches with extremely rare distribution on earth (defined as phyla with 5 genomes or less in GTDB) have been identified consistently in anaerobic habitats.

In summary, by examining microbial diversity in Zodletone spring, we greatly expand the overall diversity within the tree of life via the discovery and characterization of a wide range of novel lineages and significantly enrich the representation of a wide range of LRD lineages. We also describe a unique sulfur-cycling community in the spring that is largely dependent on sulfite, thiosulfate, sulfur, and tetrathionate, rather than sulfate, as an electron acceptor. Given the remarkable similarity to conditions prevailing prior to the GOE, we consider the spring an invaluable portal with which to investigate the community thriving on the earth's surface during these eras and posit that GOE precipitated the near extinction of a wide range of phylogenetically distinct oxygen-sensitive lineages and drastically altered the reductive sulfur-cycling community from sulfite, sulfur, and thiosulfate reducers to predominantly sulfate reduction in the current earth.

MATERIALS AND METHODS

Site description and geochemistry. Zodletone spring is located in the Anadarko Basin of western Oklahoma (N34.99562° W98.68895°). The spring arises from underground, where water is pumped out slowly along with sediments. Sediments settled at the source of the spring, a boxed square of 1 m² (Fig. S1), are overlaid with water that collects and settles in a concrete pool erected in the early 1900s. The settled water is 50 cm deep above the sediments and is exposed to atmospheric air. Water and sediments originating from the spring source are highly reduced due to the high dissolved sulfide levels (8 to 10 mM) in the spring sediments. Microsensor measurements show a completely anoxic (oxygen levels of <0.1 μM) and highly reduced source sediments. Oxygen levels slowly increase in the overlaid water column from 2 to 4 μM in the 2 mm above the source to complete oxygen exposure at the top of the water column (19). The spring geochemistry has been monitored regularly during the last 2 decades (19, 20, 71) and is remarkably stable. The spring is characterized by low levels of sulfate (50 to 94 μM), with higher levels of sulfite (0.21 mM), elemental sulfur (0.1 mM), and thiosulfate (0.52 mM) (21, 71).

Sampling. Samples were collected from the source sediments and standing overlaid water in sterile containers and kept on ice until they were transported to the lab (~2-h drive), where they were processed immediately. For metatranscriptomics, samples were collected at three different time points, namely, morning (9:15 a.m.), afternoon (2:30 p.m.), and evening (5:30 p.m.) in June 2019. They were stored on dry ice and then transferred to the lab where they were stored at -80°C until being processed for RNA extraction within a week.

Nucleic acid extraction. DNA was extracted directly from 0.5 g of source sediments. For water samples, water was filtered on 0.2-μm sterile filters. DNA was directly extracted from filters (20 filters, 10 L of water samples). Extraction was conducted using the DNeasy PowerSoil kit (Qiagen, Valencia, CA, USA). RNA was extracted from 0.5-g sediment samples using RNeasy PowerSoil total RNA kit (Qiagen) according to the manufacturer's instructions.

16S rRNA gene amplification, sequencing, and analysis. Triplicate DNA extractions were performed for both sediment and water samples from the Zodletone spring. To characterize the microbial diversity based on 16S rRNA gene sequences, we used the Quick-16S next-generation sequencing (NGS) library prep kit (Zymo Research, Irvine CA), following the manufacturer's protocol. For amplification of the V4 hypervariable region, we used a mix of modified versions of primers 515F-806R (72), tailored to provide better coverage for several underrepresented microbial lineages. They included 515FY (5'-GTGYCAGCMGCCGCGGTAA) (73), 515F-Cren (5'-GTGKACAGCMGCCGCGGTAA, for *Crenarchaeota*) (74), 515F-Nano (5'-GTGGCAGYCGCCRCGGKAA, for *Nanoarchaeota*) (74), and 515F-TM7 (5'-GTGCCAGCMGCCGCGGTCA for TM7/*Saccharibacteria*) (75) as forward mix and 805RB (5'-GGACTACNVGGGTWTCTAAT) (76) and 805R-Nano (5'-GGAMTACHGGGTCTCTAAT, for *Nanoarchaeota*) (74) as reverse mix. Purified barcoded amplicon libraries were sequenced on a MiSeq instrument (Illumina Inc., San Diego, CA) using a v2 500-cycle kit, according to the manufacturer's protocol. Demultiplexed forward

and reverse reads were imported as paired fastq files into QIIME2 v. 2020.8 (77) for analysis. The DADA2 plugin was used to trim, denoise, pair, purge chimeras, and select amplicon sequence variants (ASVs), using the command “qiime dada2 denoise-paired.” Between 44,000 and 194,000 nonchimeric sequences were obtained for the individual samples. The ASVs were classified taxonomically in QIIME2 using a trained classifier built based on the Silva-138-99 rRNA sequence database. The ASVs were assigned to 1,643 taxonomic categories corresponding to taxonomic level 7 (species and above) and to 932 genera (level 6). Alpha rarefaction curves indicated a saturation of observed sequence features (ASVs) at a sequencing depth of 70,000 to 80,000 sequences.

Metagenome sequencing, assembly, and binning. Metagenomic sequencing was conducted using the services of a commercial provider (Novogene, Beijing, China) using two lanes of the Illumina HiSeq 2500 system for each of the water and sediment samples. Transcriptomic sequencing using Illumina HiSeq 2500 2 × 150-bp paired-end technology was conducted using the services of a commercial provider (Novogene Corporation). Metagenomic reads were assessed for quality using FastQC followed by quality filtering and trimming using Trimmomatic v.0.38 (78). High-quality reads were assembled into contigs using MegaHit (v.1.1.3) with minimum kmer of 27, maximum kmer of 127, kmer step of 10, and minimum contig length of 1,000 bp. Bowtie2 was used to calculate sequencing coverage of each contig by mapping the raw reads back to the contigs. Assembled contigs were searched for ribosomal protein S3 (rpS3) sequences using a custom hidden Markov model (HMM) built from Uniprot reference sequences assigned to the KEGG orthologies (Kos) [K02982](#) and [K02984](#) (corresponding to the bacterial, and archaeal RPS3, respectively) using hmmbuild (HMMER 3.1b2). rpS3 sequences were clustered at 99% identity (ID) using CD-HIT as suggested previously for a putative species cutoff for rpS3 data (79). Taxonomic affiliations of rpS3 groups were identified using Diamond BLAST against the GTDB r95 database (24).

Contigs from the sediment and water assemblies were binned into draft genomes using both Metabat (80) and MaxBin2 (81). DasTool was used to select the highest quality bins from each metagenome assembly (82). CheckM was used for the estimation of genome completeness, strain heterogeneity, and contamination (83). Genomic bins showing contamination levels higher than 10% were further refined based on the taxonomic affiliations of the binned contigs, as well as the GC content, tetranucleotide frequency, and coverage levels using RefineM (84). Low-quality bins (>10% contamination) were cleaned by removal of the identified outlier contigs, and the percentage completeness and contamination were again rechecked using CheckM.

Genome classification, annotation, and metabolic analysis. Taxonomic classifications followed the Genome Taxonomy Database (GTDB) release r95 (24) and were carried out using the `classify_workflow` in GTDB-Tk (v.1.1.0) (85). Phylogenomic analysis utilized the concatenated alignment of a set of 120 single-copy bacterial genes and 122 single-copy archaeal genes (24) generated by the GTDB-Tk. A maximum-likelihood phylogenomic tree was constructed in FastTree using the default parameters (86).

Annotation and metabolic analysis. Protein-coding genes were predicted using Prodigal (87). GhostKOALA (88) was used for the functional annotation of every predicted open reading frame in every genomic bin and to assign protein-coding genes to KEGG orthologies (KOs).

Analysis of sulfur-cycling genes. To identify taxa mediating key sulfur-transformation processes in the spring sediments, we mapped the distribution of key sulfur-cycling genes in all genomes and deduced capacities in individual genomes by documenting the occurrence of entire pathways (as explained below in detail). This information was confirmed subsequently by phylogenetic analysis and examining contiguous gene organization in processes requiring a multisubunit and/or multigene. Furthermore, expression data were used from three time points to identify the fraction of the community that is metabolically actively involved in the process. An analysis of Sulfur (S) cycling capabilities was conducted on individual genomic bins by building and scanning hidden Markov model (HMM) profiles as explained below. To build the sulfur gene HMM profiles, Uniprot reference sequences for all genes with an assigned KO number were downloaded and aligned using Clustal Omega (89), and the alignment was used to build an HMM profile using hmmbuild (HMMER 3.1b2) (90). For genes not assigned a KO number (e.g., *otr*, *tsdA*, and *tetH*), a representative protein was compared against the KEGG database using BLASTP, and significant hits (those with E values of <e-80) were downloaded and used to build HMM profiles as explained above. The custom-built HMM profiles were then used to scan the analyzed genomes for significant hits using hmscan (HMMER 3.1b2) (90) with the option -T 100 to limit the results to only those profiles with an alignment score of at least 100. Further confirmation was achieved through phylogenetic assessment and tree building procedures, in which potential candidates identified by hmscan were aligned to the reference sequences used to build the custom HMM profiles using Clustal Omega (89), followed by maximum likelihood phylogenetic tree construction using FastTree (86). Only candidates clustering with reference sequences were deemed true hits and were assigned to the corresponding KO. Details on the genes examined for evidence of sulfate, sulfite, polysulfide, tetrathionate, and thiosulfate reduction; thiosulfate disproportionation; and various sulfur oxidation capacities are provided in the supplemental material (Text S1).

Phylogenetic analysis and operon organization of S cycling genes. The phylogenetic affiliation of the S cycling proteins AsrB, Otr, PhsC, PsrC, and DsrAB was examined by aligning the Zodletone genome predicted protein sequences to Uniprot reference sequences using MAFFT (91). The DsrA and DsrB alignments were concatenated in MEGA X (92). All alignments were used to construct maximum likelihood phylogenetic trees in RAXML (93). The R package genoPlotR (94) was used to produce gene maps for the DSR and ASR loci in Zodletone genomes using the Prodigal predicted gene starts, ends, and strand direction.

Transcription of sulfur-cycling genes. A total of 21.4 million, 27.9 million, and 22.5 million 150-bp paired-end reads were obtained from the morning, afternoon, and evening transcriptome sequencing (RNA-seq) libraries. Reads were pseudoaligned to all Prodigal-predicted genes from all genomes using Kallisto with default settings (95). The calculated transcripts per million (TPM) were used to obtain total transcription levels for genes identified from genomic analysis as involved in S cycling in the spring.

Additional metabolic analysis. For all other non-sulfur-related functional predictions, combined GhostKOALA outputs of all genomes belonging to a certain order (for orders with 5 genomes or less; $n = 206$) or family (for orders with more than 5 genomes; $n = 85$) were checked for the presence of groups of KOs constituting metabolic pathways (https://github.com/nohayoussef/Zodletone_Metagenomics). The list of these 291 lineages is shown in Table S3. The presence of at least 80% of KOs assigned to a certain pathway in at least one genome belonging to a certain order/family was used as an indication of the presence of that pathway in that order/family. Such criteria were used for the prediction of autotrophic capabilities, as well as catabolic heterotrophic degradation capabilities of sugars, amino acids, long-chain fatty acids, short-chain fatty acids, anaerobic benzoate degradation, anaerobic short-chain alkane degradation, aerobic respiration, nitrate reduction, nitrification, and chlorophyll biosynthesis. Glycolytic and fermentation capabilities were predicted by feeding the GhostKOALA output to KeggDecoder (96). Proteases, peptidases, and protease inhibitors were identified using BLASTP against the MEROPS database (97), while CAZymes (glycoside hydrolases [GHs], polysaccharide lyases [PLs], and carbohydrate esterases [CEs]) were identified by searching all open reading frames (ORFs) from all genomes against the dbCAN hidden Markov model v9 (98) (downloaded from the dbCAN Web server in September 2020) using hmmscan. FeGenie (99) was used to predict the presence of iron reduction and iron oxidation genes in individual bins.

Data availability. The whole-genome shotgun project was submitted to GenBank under BioProject identifier (ID) [PRJNA690107](https://www.ncbi.nlm.nih.gov/bioproject/PRJNA690107) and BioSample IDs [SAMN17269717](https://www.ncbi.nlm.nih.gov/biosample/SAMN17269717) (for the sediment metagenome) and [SAMN17269718](https://www.ncbi.nlm.nih.gov/biosample/SAMN17269718) (for the water metagenome). The individual assembled MAGs have been deposited at DDBJ/ENA/GenBank under accession numbers [JAFFZZ000000000](https://www.ncbi.nlm.nih.gov/nuccore/JAFFZZ000000000) to [JAFGPI000000000](https://www.ncbi.nlm.nih.gov/nuccore/JAFGPI000000000). The versions described in this paper are the first versions, [JAFFZZ010000000](https://www.ncbi.nlm.nih.gov/nuccore/JAFFZZ010000000) to [JAFGPI010000000](https://www.ncbi.nlm.nih.gov/nuccore/JAFGPI010000000). Metagenomic raw reads for the sediment and the water are available under SRA accession numbers [SRX9813571](https://www.ncbi.nlm.nih.gov/sra/SRX9813571) and [SRX9813572](https://www.ncbi.nlm.nih.gov/sra/SRX9813572). RNA-seq reads generated in this study are available under SRA accession numbers [SRX9810743](https://www.ncbi.nlm.nih.gov/sra/SRX9810743), [SRX9810744](https://www.ncbi.nlm.nih.gov/sra/SRX9810744), and [SRX9810745](https://www.ncbi.nlm.nih.gov/sra/SRX9810745) for the morning, afternoon, and evening samples, respectively.

SUPPLEMENTAL MATERIAL

Supplemental material is available online only.

TEXT S1, DOCX file, 0.1 MB.

FIG S1, PDF file, 0.1 MB.

FIG S2, PDF file, 0.04 MB.

FIG S3, PDF file, 0.2 MB.

FIG S4, PDF file, 1.8 MB.

FIG S5, PDF file, 2.3 MB.

FIG S6, PDF file, 2 MB.

TABLE S1, XLSX file, 0.1 MB.

TABLE S2, XLSX file, 0.1 MB.

TABLE S3, XLSX file, 0.1 MB.

ACKNOWLEDGMENTS

This work was supported by the National Science Foundation grants 2016423 (to N.H.Y. and M.S.E.) and 2016371 to M.P.

REFERENCES

- Jørgensen BB, Findlay AJ, Pellerin A. 2019. The biogeochemical sulfur-cycle in marine sediments. *Front Microbiol* 10:849. <https://doi.org/10.3389/fmicb.2019.00849>.
- Wasmund K, Mußmann M, Loy A. 2017. The life sulfuric: microbial ecology of sulfur cycling in marine sediments. *Environ Microbiol Rep* 9:323–344. <https://doi.org/10.1111/1758-2229.12538>.
- Vliet DM, Meijerfeldt FAB, Dutilh BE, Villanueva L, Sinninghe Damsté JS, Stams AJM, Sánchez-Andrea I. 2021. The bacterial sulfur cycle in expanding dysoxic and euxinic marine waters. *Environ Microbiol* 23:2834–2857. <https://doi.org/10.1111/1462-2920.15265>.
- Holmer M, Storkholm P. 2001. Sulphate reduction and sulphur cycling in lake sediments: a review. *Freshw Biol* 46:431–451. <https://doi.org/10.1046/j.1365-2427.2001.00687.x>.
- Schmalenberger A, Drake HL, Küsel K. 2007. High unique diversity of sulfate-reducing prokaryotes characterized in a depth gradient in an acidic fen. *Environ Microbiol* 9:1317–1328. <https://doi.org/10.1111/j.1462-2920.2007.01251.x>.
- Gieg LM, Davidova IA, Duncan KE, Suflita JM. 2010. Methanogenesis, sulfate reduction and crude oil biodegradation in hot Alaskan oilfields. *Environ Microbiol* 12:3074–3086. <https://doi.org/10.1111/j.1462-2920.2010.02282.x>.
- Steudel R. 1996. Mechanism for the formation of elemental sulfur from aqueous sulfide in chemical and microbiological desulfurization processes. *Ind Eng Chem Res* 35:1417–1423. <https://doi.org/10.1021/ie950558t>.
- Jelen B, Giovannelli D, Falkowski PG, Vetriani C. 2018. Elemental sulfur reduction in the deep-sea vent thermophile, *Thermovibrio ammonificans*. *Environ Microbiol* 20:2301–2316. <https://doi.org/10.1111/1462-2920.14280>.
- Zopfi J, Ferdelman TG, Fossing H. 2004. Distribution and fate of sulfur intermediates - sulfite, tetrathionate, thiosulfate, and elemental sulfur in marine sediments, p 97–116. *In* Amend JP, Edwards KJ, Lyons TW (ed), *Sulfur biogeochemistry—past and present*. Geological Society of America, Boulder, CO.

10. Mandal M, Bhattacharya S, Roy C, Rameez MJ, Sarkar J, Mapder T, Fernandes S, Peketi A, Mazumdar A, Ghosh W. 2020. Cryptic roles of tetrathionate in the sulfur cycle of marine sediments: microbial drivers and indicators. *Biogeosciences* 17:4611–4631. <https://doi.org/10.5194/bg-17-4611-2020>.
11. Canfield DE, Habicht KS, Thamdrup B. 2000. The Archean sulfur cycle and the early history of atmospheric oxygen. *Science* 288:658–661. <https://doi.org/10.1126/science.288.5466.658>.
12. Ranjan S, Todd ZR, Sutherland JD, Sasselov DD. 2018. Sulfidic anion concentrations on early earth for surficial origins-of-life chemistry. *Astrobiol* 18:1023–1041. <https://doi.org/10.1089/ast.2017.1770>.
13. Canfield DE, Raiswell R. 1999. The evolution of the sulfur-cycle. *Am J Sci* 299:697–723. <https://doi.org/10.2475/ajs.299.7-9.697>.
14. Habicht KS, Gade M, Thamdrup B, Berg P, Canfield DE. 2002. Calibration of sulfate levels in the Archean ocean. *Science* 298:2372–2374. <https://doi.org/10.1126/science.1078265>.
15. Habicht KS, Canfield DE, Rethmeier J. 1998. Sulfur isotope fractionation during bacterial reduction and disproportionation of thiosulfate and sulfite. *Geochim et Cosmochim Acta* 62:2585–2595. [https://doi.org/10.1016/S0016-7037\(98\)00167-7](https://doi.org/10.1016/S0016-7037(98)00167-7).
16. Philippot P, Zuilen MV, Lepot K, Thomazo C, Farquhar J, Kranendonk MJV. 2007. Early archaean microorganisms preferred elemental sulfur, not sulfide. *Science* 317:1534–1537. <https://doi.org/10.1126/science.1145861>.
17. Marin J, Battistuzzi FU, Brown AC, Hedges SB. 2017. The timetree of Prokaryotes: new insights into their evolution and speciation. *Mol Biol Evol* 34:437–446. <https://doi.org/10.1093/molbev/msw245>.
18. van der Valk T, Pečnerová P, Díez-Del-Molino D, Bergström A, Oppenheimer J, Hartmann S, Xenikoudakis G, Thomas JA, Dehasque M, Sağlıcan E, Fidan FR, Barnes I, Liu S, Somel M, Heintzman PD, Nikolskiy P, Shapiro B, Skoglund P, Hofreiter M, Lister AM, Götherström A, Dalén L. 2021. Million-year-old DNA sheds light on the genomic history of mammoths. *Nature* 591:265–269. <https://doi.org/10.1038/s41586-021-03224-9>.
19. Buhning SI, Sievert SM, Jonkers HM, Ertefai T, Elshahed MS, Krumholz LR, Hinrichs K-U. 2011. Insights into chemotaxonomic composition and carbon cycling of phototrophic communities in an artesian sulfur-rich spring (Zodletone, Oklahoma, USA), a possible analog for ancient microbial mat systems. *Geobiology* 9:166–179. <https://doi.org/10.1111/j.1472-4669.2010.00268.x>.
20. Elshahed MS, Senko JM, Najjar FZ, Kenton SM, Roe BA, Dewers TA, Spear JR, Krumholz LR. 2003. Bacterial diversity and sulfur cycling in a mesophilic sulfide-rich spring. *Appl Environ Microbiol* 69:5609–5621. <https://doi.org/10.1128/AEM.69.9.5609-5621.2003>.
21. Spain AM, Elshahed MS, Najjar FZ, Krumholz LR. 2015. Metatranscriptomic analysis of a high-sulfide aquatic spring reveals insights into sulfur cycling and unexpected aerobic metabolism. *PeerJ* 3:e1259. <https://doi.org/10.7717/peerj.1259>.
22. Youssef N, Steidley BL, Elshahed MS. 2012. Novel high-rank phylogenetic lineages within a sulfur spring (Zodletone Spring, Oklahoma), revealed using a combined pyrosequencing-sanger approach. *Appl Environ Microbiol* 78:2677–2688. <https://doi.org/10.1128/AEM.00002-12>.
23. Youssef NH, Couger MB, Elshahed MS. 2010. Fine-scale bacterial beta diversity within a complex ecosystem (Zodletone Spring, OK, USA): the role of the rare biosphere. *PLoS One* 5:e12414. <https://doi.org/10.1371/journal.pone.0012414>.
24. Parks DH, Chuvochina M, Chaumeil P-A, Rinke C, Mussig AJ, Hugenholtz P. 2020. A complete domain-to-species taxonomy for Bacteria and Archaea. *Nat Biotechnol* 38:1079–1086. <https://doi.org/10.1038/s41587-020-0501-8>.
25. Nayfach S, Roux S, Seshadri R, Udway D, Varghese N, Schulz F, Wu D, Paez-Espino D, Chen IM, Huntemann M, Palaniappan K, Ladau J, Mukherjee S, Reddy TBK, Nielsen T, Kirton E, Faria JP, Edirisinghe JN, Henry CS, Jungbluth SP, Chivian D, Dehal P, Wood-Charlson EM, Arkin AP, Tringe SG, Visel A, Woyke T, Mouncey NJ, Ivanova NN, Kyrpidis NC, Eloe-Fadrosh EA, IMG/M Data Consortium. 2021. A genomic catalog of Earth's microbiomes. *Nat Biotechnol* 39:520. <https://doi.org/10.1038/s41587-020-00769-4>.
26. Vavourakis CD, Mehrshad M, Balkema C, Hall R, Andrei A-S, Ghai R, Sorokin DY, Muyzer G. 2019. Metagenomes and metatranscriptomes shed new light on the microbial-mediated sulfur cycle in a Siberian soda lake. *BMC Microbiol* 17:69. <https://doi.org/10.1186/s12915-019-0688-7>.
27. Price-Carter M, Tingey J, Bobik TA, Roth JR. 2001. The alternative electron acceptor tetrathionate supports B12-dependent anaerobic growth of *Salmonella enterica* serovar typhimurium on ethanolamine or 1,2-propanediol. *J Bacteriol* 183:2463–2475. <https://doi.org/10.1128/JB.183.8.2463-2475.2001>.
28. Finster K, Liesack W, Thamdrup B. 1998. Elemental sulfur and thiosulfate disproportionation by *Desulfocapsa sulfoexigens* sp. nov., a new anaerobic bacterium isolated from marine surface sediment. *Appl Environ Microbiol* 64:119–125. <https://doi.org/10.1128/AEM.64.1.119-125.1998>.
29. Jackson BE, McInerney MJ. 2000. Thiosulfate disproportionation by *Desulfotomaculum thermobenzoicum*. *Appl Environ Microbiol* 66:3650–3653. <https://doi.org/10.1128/AEM.66.8.3650-3653.2000>.
30. Aird BA, Heinrich RL, Westley J. 1987. Isolation and characterization of a prokaryotic sulfurtransferase. *J Biol Chem* 262:17327–17335. [https://doi.org/10.1016/S0021-9258\(18\)45381-1](https://doi.org/10.1016/S0021-9258(18)45381-1).
31. Etchebere C, Muxí L. 2000. Thiosulfate reduction and alanine production in glucose fermentation by members of the genus *Coprothermobacter*. *Antonie Van Leeuwenhoek* 77:321–327. <https://doi.org/10.1023/a:1002636212991>.
32. Kaji A, Mc EW. 1959. Mechanism of hydrogen sulfide formation from thiosulfate. *J Bacteriol* 77:630–637. <https://doi.org/10.1128/jb.77.5.630-637.1959>.
33. Peck HD, Jr, Fisher E, Jr. 1962. The oxidation of thiosulfate and phosphorylation in extracts of *Thiobacillus thioautotrophicus*. *J Biol Chem* 237:190–197. [https://doi.org/10.1016/S0021-9258\(18\)81384-9](https://doi.org/10.1016/S0021-9258(18)81384-9).
34. Ravot G, Ollivier B, Magot M, Patel B, Crolet J, Fardeau M, Garcia J. 1995. Thiosulfate reduction, an important physiological feature shared by members of the order Thermotogales. *Appl Environ Microbiol* 61:2053–2055. <https://doi.org/10.1128/aem.61.5.2053-2055.1995>.
35. Kanao T, Kamimura K, Sugio T. 2007. Identification of a gene encoding a tetrathionate hydrolase in *Acidithiobacillus ferrooxidans*. *J Biotechnol* 132:16–22. <https://doi.org/10.1016/j.jbiotec.2007.08.030>.
36. Achtnich C, Bak F, Conrad R. 1995. Competition for electron donors among nitrate reducers, ferric iron reducers, sulfate reducers, and methanogens in anoxic paddy soil. *Biol Fertil Soils* 19:65–72. <https://doi.org/10.1007/BF00336349>.
37. Glombitza C, Egger M, Røy H, Jørgensen BB. 2019. Controls on volatile fatty acid concentrations in marine sediments (Baltic Sea). *Geochim et Cosmochim Acta* 258:226–241. <https://doi.org/10.1016/j.gca.2019.05.038>.
38. Morrison JM, Baker KD, Zamor RM, Nikolai S, Elshahed MS, Youssef NH. 2017. Spatiotemporal analysis of microbial community dynamics during seasonal stratification events in a freshwater lake (Grand Lake, OK, USA). *PLoS One* 12:e0177488. <https://doi.org/10.1371/journal.pone.0177488>.
39. Daly RA, Borton MA, Wilkins MJ, Hoyt DW, Kountz DJ, Wolfe RA, Welch SA, Marcus DN, Trexler RV, MacRae JD, Krzycki JA, Cole DR, Mouser PJ, Wrighton KC. 2016. Microbial metabolisms in a 2.5-km-deep ecosystem created by hydraulic fracturing in shales. *Nature Microbiol* 1:16146. <https://doi.org/10.1038/nmicrobiol.2016.146>.
40. Jørgensen BB, Marshall IPG. 2016. Slow microbial life in the seabed. *Annu Rev Mar Sci* 8:311–332. <https://doi.org/10.1146/annurev-marine-010814-015535>.
41. Jørgensen BB, Isaksen MF, Jannasch HW. 1992. Bacterial sulfate reduction above 100°C in deep-sea hydrothermal vent sediments. *Science* 258:1756–1757. <https://doi.org/10.1126/science.258.5089.1756>.
42. Scholze C, Jørgensen BB, Roy H. 2020. Psychrophilic properties of sulfate-reducing bacteria in Arctic marine sediments. *Limnol Oceanogr* 66:5293–5302. <https://doi.org/10.1002/lno.11586>.
43. Sánchez-Andrea I, Sanz JL, Bijmans MF, Stams AJ. 2014. Sulfate reduction at low pH to remediate acid mine drainage. *J Hazard Mater* 269:98–109. <https://doi.org/10.1016/j.jhazmat.2013.12.032>.
44. Sorokin DY, Kuenen JG, Muyzer G. 2011. The microbial sulfur cycle at extremely haloalkaline conditions of soda lakes. *Front Microbiol* 2:44. <https://doi.org/10.3389/fmicb.2011.00044>.
45. Teske A, Ramsing NB, Habicht K, Fukui M, Küver J, Jørgensen BB, Cohen Y. 1998. Sulfate-reducing bacteria and their activities in cyanobacterial mats of Solar Lake (Sinai, Egypt). *Appl Environ Microbiol* 64:2943–2951. <https://doi.org/10.1128/AEM.64.8.2943-2951.1998>.
46. Bell E, Lamminmäki T, Alneberg J, Andersson AF, Qian C, Xiong W, Hettich RL, Fruttschi M, Bernier-Latmani R. 2020. Active sulfur cycling in the terrestrial deep subsurface. *ISME J* 14:1260–1272. <https://doi.org/10.1038/s41396-020-0602-x>.
47. Rabus R, Venceslau SS, Wöhlbrand L, Voordouw G, Wall JD, Pereira IA. 2015. A post-genomic view of the ecophysiology, catabolism and biotechnological relevance of sulphate-reducing prokaryotes. *Adv Microb Physiol* 66:55–321. <https://doi.org/10.1016/bs.ampbs.2015.05.002>.
48. Bertran E, Leavitt WD, Pellerin A, Zane GM, Wall JD, Halevy I, Wing BA, Johnston DT. 2018. Deconstructing the dissimilatory sulfate reduction

- pathway: isotope fractionation of a mutant unable of growth on sulfate. *Front Microbiol* 9:3110. <https://doi.org/10.3389/fmicb.2018.03110>.
49. Peck HD, Jr, LeGall J. 1982. Biochemistry of dissimilatory sulphate reduction. *Philos Trans R Soc Lond B Biol Sci* 298:443–466.
 50. Wenk CB, Wing BA, Halevy I. 2018. Electron carriers in microbial sulfate reduction inferred from experimental and environmental sulfur isotope fractionations. *ISME J* 12:495–507. <https://doi.org/10.1038/ismej.2017.185>.
 51. Rabus R, Hansen TA, Widdel F. 2013. Dissimilatory sulfate- and sulfur-reducing prokaryotes, p 309–404. In Rosenberg E, DeLong EF, Lory S, Stackebrandt E, Thompson F (ed), *The prokaryotes: prokaryotic physiology and biochemistry*. Springer Berlin Heidelberg, Berlin, Germany.
 52. Anantharaman K, Hausmann B, Jungbluth SP, Kantor RS, Lavy A, Warren LA, Rappé MS, Pester M, Loy A, Thomas BC, Banfield JF. 2018. Expanded diversity of microbial groups that shape the dissimilatory sulfur cycle. *ISME J* 12:1715–1728. <https://doi.org/10.1038/s41396-018-0078-0>.
 53. Hausmann B, Pelikan C, Herbold CW, Köstlbacher S, Albertsen M, Eichorst SA, Glavina Del Rio T, Huemer M, Nielsen PH, Rattei T, Stingl U, Tringe SG, Trojan D, Wentrup C, Woebken D, Pester M, Loy A. 2018. Peatland Acidobacteria with a dissimilatory sulfur metabolism. *ISME J* 12:1729–1742. <https://doi.org/10.1038/s41396-018-0077-1>.
 54. Flieder M, Buongiorno J, Herbold CW, Hausmann B, Rattei T, Lloyd KG, Loy A, Wasmund K. 2021. Novel taxa of Acidobacteriota involved in sea-floor sulfur cycling. *ISME J* 15:3159–3180. <https://doi.org/10.1038/s41396-021-00992-0>.
 55. Villemur R, Lanthier M, Beaudet R, Lépine F. 2006. The *Desulfitobacterium* genus. *FEMS Microbiol Rev* 30:706–733. <https://doi.org/10.1111/j.1574-6976.2006.00029.x>.
 56. Huang CJ, Barrett EL. 1991. Sequence analysis and expression of the *Salmonella typhimurium* *asr* operon encoding production of hydrogen sulfide from sulfite. *J Bacteriol* 173:1544–1553. <https://doi.org/10.1128/jb.173.4.1544-1553.1991>.
 57. Shirodkar S, Reed S, Romine M, Saffarini D. 2011. The octahaem SirA catalyses dissimilatory sulfite reduction in *Shewanella oneidensis* MR-1. *Environ Microbiol* 13:108–115. <https://doi.org/10.1111/j.1462-2920.2010.02313.x>.
 58. Kern M, Klotz MG, Simon J. 2011. The *Wolinella succinogenes* *mcc* gene cluster encodes an unconventional respiratory sulphite reduction system. *Mol Microbiol* 82:1515–1530. <https://doi.org/10.1111/j.1365-2958.2011.07906.x>.
 59. Colman DR, Lindsay MR, Amenabar MJ, Fernandes-Martins MC, Roden ER, Boyd ES. 2020. Phylogenomic analysis of novel *Diaphorarchaea* is consistent with sulfite but not sulfate reduction in volcanic environments on early Earth. *ISME J* 14:1316–1331. <https://doi.org/10.1038/s41396-020-0611-9>.
 60. Frederiksen TM, Finster K. 2003. Sulfite-oxido-reductase is involved in the oxidation of sulfite in *Desulfocapsa sulfoexigens* during disproportionation of thiosulfate and elemental sulfur. *Biodegradation* 14:189–198. <https://doi.org/10.1023/a:1024255830925>.
 61. Sun B, Cole JR, Tiedje JM. 2001. *Desulfomonile limimaris* sp. nov., an anaerobic dehalogenating bacterium from marine sediments. *Int J Syst Evol Microbiol* 51:365–371. <https://doi.org/10.1099/00207173-51-2-365>.
 62. Townsend GT, Sulflita JM. 1997. Influence of sulfur oxyanions on reductive dehalogenation activities in *Desulfomonile tiedjei*. *Appl Environ Microbiol* 63:3594–3599. <https://doi.org/10.1128/aem.63.9.3594-3599.1997>.
 63. Haschke RH, Campbell LL. 1971. Thiosulfate reductase of *Desulfovibrio vulgaris*. *J Bacteriol* 106:603–607. <https://doi.org/10.1128/jb.106.2.603-607.1971>.
 64. Obratzsova AY, Francis CA, Tebo BM. 2002. Sulfur disproportionation by the facultative anaerobe *Pantoea agglomerans* SP1 as a mechanism for Chromium(VI) reduction. *Geomicrobiol J* 19:121–132. <https://doi.org/10.1080/014904502317246219>.
 65. Mardanov AV, Beletsky AV, Kadnikov VV, Slobodkin AI, Ravin NV. 2016. Genome analysis of *Thermosulfurimonas dismutans*, the first thermophilic sulfur-disproportionating bacterium of the phylum *Thermodesulfobacteria*. *Front Microbiol* 7:950. <https://doi.org/10.3389/fmicb.2016.00950>.
 66. Jørgensen BB. 1990. A thiosulfate shunt in the sulfur cycle of marine sediments. *Science* 249:152–154. <https://doi.org/10.1126/science.249.4965.152>.
 67. Jørgensen BB. 1990. The sulfur cycle of freshwater sediments: role of thiosulfate. *Limnol Oceanogr* 35:1329–1342. <https://doi.org/10.4319/lo.1990.35.6.1329>.
 68. Lyons TW, Reinhard CT, Planavsky NJ. 2014. The rise of oxygen in Earth's early ocean and atmosphere. *Nature* 506:307–315. <https://doi.org/10.1038/nature13068>.
 69. Killingsworth BA, Sansjofre P, Philippot P, Cartigny P, Thomazo C, Lalonde V. 2019. Constraining the rise of oxygen with oxygen isotopes. *Nature Comm* 10:4924. <https://doi.org/10.1038/s41467-019-12883-2>.
 70. Holland HD. 1965. Some applications of thermochemical data to problems of ore deposits; part 2, mineral assemblages and the composition of ore forming fluids. *Econ Geol* 60:1101–1166. <https://doi.org/10.2113/gsecongeo.60.6.1101>.
 71. Senko JM, Campbell BS, Henriksen JR, Elshahed MS, Dewers TA, Krumholz LR. 2004. Barite deposition mediated by phototrophic sulfide-oxidizing bacteria. *Geochim Cosmochim Acta* 68:773–780. <https://doi.org/10.1016/j.gca.2003.07.008>.
 72. Caporaso JG, Lauber CL, Walters WA, Berg-Lyons D, Lozupone CA, Turnbaugh PJ, Fierer N, Knight R. 2011. Global patterns of 16S rRNA diversity at a depth of millions of sequences per sample. *Proc Natl Acad Sci U S A* 108:4516–4522. <https://doi.org/10.1073/pnas.1000080107>.
 73. Parada AE, Needham DM, Fuhrman JA. 2016. Every base matters: assessing small subunit rRNA primers for marine microbiomes with mock communities, time series and global field samples. *Environ Microbiol* 18:1403–1414. <https://doi.org/10.1111/1462-2920.13023>.
 74. Podar PT, Yang Z, Björnsdóttir SH, Podar M. 2020. Comparative analysis of microbial diversity across temperature gradients in hot springs from Yellowstone and Iceland. *Front Microbiol* 11:1625. <https://doi.org/10.3389/fmicb.2020.01625>.
 75. Cross KL, Campbell JH, Balachandran M, Campbell AG, Cooper SJ, Griffen A, Heaton M, Joshi S, Klingeman D, Leys E, Yang Z, Parks JM, Podar M. 2019. Targeted isolation and cultivation of uncultivated bacteria by reverse genomics. *Nat Biotechnol* 37:1314–1321. <https://doi.org/10.1038/s41587-019-0260-6>.
 76. Walters W, Hyde ER, Berg-Lyons D, Ackermann J, Humphrey G, Parada A, Gilbert JA, Jansson JK, Caporaso JG, Fuhrman JA, Apprill A, Knight R. 2016. Improved bacterial 16S rRNA gene (V4 and V4-5) and fungal internal transcribed spacer marker gene primers for microbial community surveys. *mSystems* 1:e00009-15. <https://doi.org/10.1128/mSystems.00009-15>.
 77. Bolyen E, Rideout JR, Dillon MR, Bokulich NA, Abnet CC, Al-Ghalith GA, Alexander H, Alm EJ, Arumugam M, Asnicar F, Bai Y, Bisanz JE, Bittinger K, Brejnrod A, Brislawn CJ, Brown CT, Callahan BJ, Caraballo-Rodríguez AM, Chase J, Cope EK, Da Silva R, Diener C, Dorrestein PC, Douglas GM, Durall DM, Duvallet C, Edwardson CF, Ernst M, Estaki M, Fouquier J, Gauglitz JM, Gibbons SM, Gibson DL, Gonzalez A, Gorlick K, Guo J, Hillmann B, Holmes S, Holste H, Huttenhower C, Huttley GA, Janssen S, Jarmusch AK, Jiang L, Kaehler BD, Kang KB, Keefe CR, Keim P, Kelley ST, Knights D, et al. 2019. Reproducible, interactive, scalable and extensible microbiome data science using QIIME 2. *Nat Biotechnol* 37:852–857. <https://doi.org/10.1038/s41587-019-0209-9>.
 78. Bolger AM, Lohse M, Usadel B. 2014. Trimmomatic: a flexible trimmer for Illumina sequence data. *Bioinformatics* 30:2114–2120. <https://doi.org/10.1093/bioinformatics/btu170>.
 79. Diamond S, Andeer PF, Li Z, Crits-Christoph A, Burstein D, Anantharaman K, Lane KR, Thomas BC, Pan C, Northen TR, Banfield JF. 2019. Mediterranean grassland soil C–N compound turnover is dependent on rainfall and depth, and is mediated by genomically divergent microorganisms. *Nat Microbiol* 4:1356–1367. <https://doi.org/10.1038/s41564-019-0449-y>.
 80. Kang DD, Li F, Kirton E, Thomas A, Egan R, An H, Wang Z. 2019. MetaBAT 2: an adaptive binning algorithm for robust and efficient genome reconstruction from metagenome assemblies. *PeerJ* 7:e7359. <https://doi.org/10.7717/peerj.7359>.
 81. Wu Y-W, Simmons BA, Singer SW. 2016. MaxBin 2.0: an automated binning algorithm to recover genomes from multiple metagenomic datasets. *Bioinformatics* 32:605–607. <https://doi.org/10.1093/bioinformatics/btv638>.
 82. Sieber CMK, Probst AJ, Sharrar A, Thomas BC, Hess M, Tringe SG, Banfield JF. 2018. Recovery of genomes from metagenomes via a dereplication, aggregation and scoring strategy. *Nat Microbiol* 3:836–843. <https://doi.org/10.1038/s41564-018-0171-1>.
 83. Parks DH, Imelfort M, Skennerton CT, Hugenholtz P, Tyson GW. 2015. CheckM: assessing the quality of microbial genomes recovered from isolates, single cells, and metagenomes. *Genome Res* 25:1043–1055. <https://doi.org/10.1101/gr.186072.114>.
 84. Parks DH, Rinke C, Chuvochina M, Chaumeil P-A, Woodcroft BJ, Evans PN, Hugenholtz P, Tyson GW. 2017. Recovery of nearly 8,000 metagenome-assembled genomes substantially expands the tree of life. *Nat Microbiol* 2:1533–1542. <https://doi.org/10.1038/s41564-017-0012-7>.
 85. Chaumeil P-A, Mussig AJ, Hugenholtz P, Parks DH. 2019. GTDB-Tk: a toolkit to classify genomes with the Genome Taxonomy Database. *Bioinformatics* 36:1925–1927. <https://doi.org/10.1093/bioinformatics/btz848>.
 86. Price MN, Dehal PS, Arkin AP. 2010. FastTree 2—approximately maximum-likelihood trees for large alignments. *PLoS One* 5:e9490. <https://doi.org/10.1371/journal.pone.0009490>.

87. Hyatt D, Chen G-L, Locascio PF, Land ML, Larimer FW, Hauser LJ. 2010. Prodigal: prokaryotic gene recognition and translation initiation site identification. *BMC Bioinformatics* 11:119. <https://doi.org/10.1186/1471-2105-11-119>.
88. Kanehisa M, Sato Y, Morishima K. 2016. BlastKOALA and GhostKOALA: KEGG tools for functional characterization of genome and metagenome sequences. *J Mol Biol* 428:726–731. <https://doi.org/10.1016/j.jmb.2015.11.006>.
89. Sievers F, Wilm A, Dineen D, Gibson TJ, Karplus K, Li W, Lopez R, McWilliam H, Remmert M, Söding J, Thompson JD, Higgins DG. 2011. Fast, scalable generation of high-quality protein multiple sequence alignments using Clustal Omega. *Mol Syst Biol* 7:539. <https://doi.org/10.1038/msb.2011.75>.
90. Mistry J, Finn RD, Eddy SR, Bateman A, Punta M. 2013. Challenges in homology search: HMMER3 and convergent evolution of coiled-coil regions. *Nucleic Acids Res* 41:e121. <https://doi.org/10.1093/nar/gkt263>.
91. Katoh K, Misawa K, Kuma K-i, Miyata T. 2002. MAFFT: a novel method for rapid multiple sequence alignment based on fast Fourier transform. *Nucleic Acids Res* 30:3059–3066. <https://doi.org/10.1093/nar/gkf436>.
92. Kumar S, Stecher G, Li M, Knyaz C, Tamura K. 2018. MEGA X: Molecular Evolutionary Genetics Analysis across computing platforms. *Mol Biol Evol* 35:1547–1549. <https://doi.org/10.1093/molbev/msy096>.
93. Kozlov AM, Darriba D, Flouri T, Morel B, Stamatakis A. 2019. RAxML-NG: a fast, scalable and user-friendly tool for maximum likelihood phylogenetic inference. *Bioinformatics* 35:4453–4455. <https://doi.org/10.1093/bioinformatics/btz305>.
94. Guy L, Kultima JR, Andersson SGE. 2010. genoPlotR: comparative gene and genome visualization in R. *Bioinformatics* 26:2334–2335. <https://doi.org/10.1093/bioinformatics/btq413>.
95. Bray NL, Pimentel H, Melsted P, Pachter L. 2016. Near-optimal probabilistic RNA-seq quantification. *Nat Biotechnol* 34:525–527. <https://doi.org/10.1038/nbt.3519>.
96. Graham ED, Heidelberg JF, Tully BJ. 2018. Potential for primary productivity in a globally-distributed bacterial phototroph. *ISME J* 12:1861–1866. <https://doi.org/10.1038/s41396-018-0091-3>.
97. Rawlings ND, Barrett AJ, Thomas PD, Huang X, Bateman A, Finn RD. 2018. The MEROPS database of proteolytic enzymes, their substrates and inhibitors in 2017 and a comparison with peptidases in the PANTHER database. *Nucleic Acids Res* 46:D624–D632. <https://doi.org/10.1093/nar/gkx1134>.
98. Huang L, Zhang H, Wu P, Entwistle S, Li X, Yohe T, Yi H, Yang Z, Yin Y. 2018. dbCAN-seq: a database of carbohydrate-active enzyme (CAZyme) sequence and annotation. *Nucleic Acids Res* 46:D516–D521. <https://doi.org/10.1093/nar/gkx894>.
99. Garber AI, Neelson KH, Okamoto A, McAllister SM, Chan CS, Barco RA, Merino N. 2020. FeGenie: a comprehensive tool for the identification of iron genes and iron gene neighborhoods in genome and metagenome assemblies. *Front Microbiol* 11:37. <https://doi.org/10.3389/fmicb.2020.00037>.